GSA Data Repository 2018104

A mineralogical signature for Burgess Shale-type fossilization

Ross P. Anderson, Nicholas J. Tosca, Robert R. Gaines, Nicolás Mongiardino Koch, and Derek E.G. Briggs

Email: ross.anderson@all-souls.ox.ac.uk

Further methodological particulars

Samples were taken from the collections of R.R. Gaines (n = 184), the Oxford University Museum of Natural History (n = 11), and the Yale Peabody Museum of Natural History (n = 18).

Matrix material was selected randomly from that immediately surrounding (i.e., within a few centimeters) the fossil (in the case of museum specimens), or from the same bed as fossiliferous material (in the case of specimens in the collection of R.R. Gaines). Samples from which BST fossils are considered absent were selected from localities where significant collection efforts have revealed no soft-bodied fossils in these particular horizons. Although absence of recovered BST fossils does not provide absolute evidence of their absence from these horizons, we compared these samples to many others in our dataset in which soft bodied fossils are conspicuous and abundant. Material was hand-ground to approximately 10 μm grain size with a porcelain pestle and mortar. Enough matrix material was ground to adequately cover single silicon crystal substrates 27 mm in diameter.

All X-ray diffraction (XRD) peak positions were adjusted to correct for slight variations in sample height displacement error using positions of quartz reflections as internal standards. Analysis of the 060 region identified other peaks in the range 1.520–1.530 Å, but their abundance was positively correlated with that of calcite obtained from the bulk analysis, consistent with the identification of variable quantities of this mineral through bulk analysis (Kendall's $\tau = 0.6344$, $P < 10^{-16}$). Additional confirmation of clay mineral species was obtained through analysis of oriented < 2 μm clay separates. Such separates were analyzed from 22 samples representing the entire suite of clay minerals observed, in order to ensure consistency in clay mineral identification with the 060 powder analysis. The mineral identifications were consistent between the two methods.

Statistical methodology

Abundance of all clay minerals showed a highly skewed zero-inflated distribution, resulting in a departure from multivariate normality, and most pairs of clay minerals proved to be significantly correlated (Fig. DR2). We therefore transformed the dataset to a matrix of pair-wise Euclidean distances between observations, and we used principal coordinate analysis (PCoA) to visualize the variability. Differences in clay mineral composition between samples with BST fossils and those with only fossil mineralized skeletons were tested using PERMANOVA (permutational multivariate analysis of variance, Anderson, 2001). Differences in the multivariate spread of both groups were tested using permutational analysis of multivariate dispersion, hereafter PERMDISP (Anderson, 2006). Both analyses were implemented using the package *vegan* (Oksanen et al., 2016), and significance was evaluated by performing 10^5 permutations.

We performed a multiple logistic regression to investigate how different clay minerals affected the probability of samples containing BST fossils. This regression used the six clay mineral abundance variables as predictors of a binary outcome: the presence of BST fossils or the presence of only fossil mineralized skeletons. The best fitting logistic model was determined using stepwise variable selection in both directions. At each step, the inclusion or exclusion of any given predictor from the model was assessed using likelihood ratio tests (LRT). The best fitting model was visualized with the package *visreg* (Breheny and Burchett, 2016).

Finally, the relationship between clay mineral composition and BST fossil-bearing samples was explored using a conditional inference classification tree (Strobl et al., 2009) built using the package *partykit* (Hothorn and Zeileis, 2015). This approach selects the predictor with the strongest association with the response variable (using Bonferroni adjusted *P* values), implements a binary split, and iterates over the newly generated subsets of data until the null hypothesis of independence cannot be rejected (Hothorn et al., 2006). This procedure guarantees unbiased variable selection and avoids overfitting (Hothorn and Zeileis, 2015).

The goodness of fit of the models derived from these two approaches (logistic regression and classification tree) was evaluated based on classification accuracy.

Independence of samples

The statistical models are all based on the assumption that each observation is independent. Many of our samples derive from stratigraphic suites from the same geological formation and locality. Clay mineral assemblages are controlled in part by the provenance of detrital clay input into a geological basin over time, and the impact of diagenesis on that detrital assemblage. Thus, the possibility that clay composition could be similar in samples from the same succession must be taken into account in interpreting the significance of the results presented here. Where multiple samples were taken from the same formation, each distinct horizon is represented by just one sample. All samples therefore derive from different depositional events, which reduces the expected dependence between samples. Furthermore, methods accommodating some lack of independence among observations from the same locality were also tested whenever possible. We ran the multiple logistic regression model using the Huber-White method (Huber, 1967; White, 1982), which adjusts the variance-covariance matrix to correct for correlated responses from clustered samples (Cameron and Miller, 2015), with formation provenance as clustering variable. This analysis supported the same results ($P \leq 0.0001$ for illite composition 1 and illite composition 2, 0.0023 for berthierine/chamosite and 0.029 for celadonite). Thus, the stratigraphic bundling of a proportion of the samples does not compromise our conclusions regarding the effect of clay minerals on organic preservation.

Absolute abundances of clays

Obtaining the absolute abundance of clay minerals within a given sample is challenging. While quantitative data can be obtained using Rietveld refinement (Snyder and Bish, 1989), such a procedure is not feasible on a sample set of this size. To obtain semi-quantitative estimates of abundances we scaled the relative clay mineral proportions from the 060 region to the total clay fraction from the bulk mineralogical analysis. This total fraction was determined by summing all identified clay mineral abundances in the bulk results and, for selected samples, checking this relationship against the total integrated area of the 020 reflection, common to all layer silicates (Środoń et al., 2001). This technique preserved the relative differences in clay content between samples.

The influence of diagenetic carbonate minerals on statistical models

There is evidence that carbonate minerals in many of these rocks are a product of early diagenesis (e.g., Gaines et al., 2012). We removed both calcite and dolomite from the mineralogical data and adjusted the abundances of the other minerals accordingly, in an attempt to better represent the original (pre-diagenetic) mineralogical composition of the samples. The

results remain robust to this adjustment: the logistic regression model is almost identical, including significant effects of illite composition 1, illite composition 2, berthierine/chamosite, and celadonite ($P = 2.2e^{-12}$, $9.4e^{-7}$, $4.8e^{-4}$, and $2.6e^{-3}$, respectively), as well as a marginally significant effect of glauconite ($P = 0.046$). Kaolinite has no effect ($P = 0.14$).

The influence of illite composition 1 and the Kaili Formation on statistical models

The abundance of illite composition 1 is a crucial factor in distinguishing samples that contain BST fossils from those that contain only fossil mineralized skeletons. Not only is it recovered by both models as the most important predictor of association with carbonaceous fossils, it is also significantly negatively correlated with the abundance of all other clay minerals (Fig. DR2). The Kaili Formation, which represents 22% of our entire dataset, is especially rich in illite composition 1, with a mean abundance of 37.9% (standard deviation = 22.8%) compared to only 2.05% (standard deviation = 10.36%) in all other samples. In order to test whether the samples from the Kaili Formation bias our results, we ran the multiple logistic regression without them. The results are robust to the removal of Kaili samples. Not only did illite composition 1 remain the most significant predictor of whether a sample would contain BST fossils, the model supported was identical, including illite composition 2, celadonite, and berthierine/chamosite ($P = 2.2e^{-6}$, $1.9e^{-7}$, $5.0e^{-3}$ and $2.4e^{-2}$, respectively). No significant effect of glauconite or kaolinite was detected ($P = 0.26$ and 0.34, respectively).

Origin of the observed clay mineral assemblage

The composition of the observed clay mineral assemblages depends on the original detrital material and the degree to which it has been transformed in response to pore water chemistry during early and/or late diagenesis (including burial metamorphism). Thus, clay mineral assemblages are prone to alteration by weathering. In fine-grained siliciclastic rocks, the mineral most susceptible to weathering is pyrite, which if chemically altered could mobilize iron and might lead to secondary precipitation of Fe-minerals such as berthierine. But Fe-oxides, and jarosite in particular, which are the major products of pyrite weathering, are absent from our samples. Kaolinite, however, is conspicuously absent even though many of these rocks were deposited at tropical paleolatitudes, further supporting a diagenetic origin for berthierine through kaolinite conversion during early and/or late diagenesis (e.g., Bhattacharyya, 1983; Taylor, 1990; Taylor and Curtis, 1995; Fritz and Toth, 1997; Toth and Fritz, 1997; Rivard et al., 2013). Where berthierine has been reported from laterites rich in kaolinite and Fe-oxides (e.g., Toth and Fritz, 1997 and references therein), these laterites have been drowned by marine transgressions, or stagnant groundwater flow has led to reductive diagenetic transformation of goethite and kaolinite to berthierine. Berthierine is not a product of the chemical weathering process *sensu stricto*, but a product derived from the reaction between Fe^{2+} and kaolinite (i.e., Bhattacharyya, 1983). This relationship also explains why the major occurrence of berthierine is in ironstones, where it alternates with glauconite as an authigenic cement (Pufahl, 2010). The diagenetic transformation of kaolinite in the presence of Fe^{2+} drives this process (demonstrated in the laboratory by Bhattacharyya, 1983): goethite and kaolinite are dominant detrital components of the tropical soils that generate the ironstones (Pufahl, 2010). We therefore do not consider weathering to have compromised our data in a significant manner, particularly in relation to the formation of berthierine.

References

Anderson, M. J., 2001, A new method for non-parametric multivariate analysis of variance: Austral Ecology, v. 26, no. 1, p. 32–46.

Anderson, M. J., 2006, Distance-based tests for homogeneity of multivariate dispersions: Biometrics, v. 62, no. 1, p. 245–253.

Bhattacharyya, D. P., 1983, Origin of berthierine in ironstones: Clays and Clay Minerals, v. 31, no. 3, p. 173–182.

Breheny, P., and Burchett, W., 2016, Visualization of Regression Models using visreg.

Cameron, A. C., and Miller, D. L., 2015, A practitioner's guide to cluster-robust inference: Journal of Human Resources, v. 50, no. 2, p. 317–372.

Fritz, S. J., and Toth, T. A., 1997, An Fe-berthierine from a Cretaceous laterite: Part II. Estimation of Eh, pH, and pCO_2 conditions of formation: Clays and Clay Minerals, v. 45, no. 4, p. 580–586.

Gaines, R. R., Hammarlund, E. U., Hou, X., Qi, C., Gabbott, S. E., Zhao, Y., Peng, J., and Canfield, D. E., 2012, Mechanism for Burgess Shale-type preservation: Proceedings of the National Academy of Sciences, v. 109, no. 14, p. 5180–5184.

Hothorn, T., Hornik, K., and Zeileis, A., 2006, Unbiased recursive partitioning: A conditional inference framework: Journal of Computational and Graphical statistics, v. 15, no. 3, p. 651–674.

Hothorn, T., and Zeileis, A., 2015, partykit: A modular toolkit for recursive partytioning in R: Journal of Machine Learning Research, v. 16, p. 3905–3909.

Huber, P. J., 1967, The behaviour of maximum likelihood estimates under nonstandard conditions: Proceedings of the fifth Berkeley symposium on mathematical statistcs and probability, p. 221–233.

Oksanen, J., Blanchet, F. G., Kindt, R., Legendre, P., Minchin, P. R., O'Hara, R. B., Simpson, G. L., Solymos, P., Stevens, M. H. H., and Wagner, H., 2016, vegan: Community Ecology Package.

Pufahl, P. K., 2010, Bioelemental sediments, Facies models 4, Volume 6, Geological Association of Canada GEOText, p. 477–503.

Rivard, C., Pelletier, M., Michau, N., Razafitianamaharevo, A., Bihannic, I., Abdelmoula, M., Ghanbaja, J., and Villéras, F., 2013, Berthierine-like mineral formation and stability during interaction of kaolinite with metallic iron at 90ºC under anoxic and oxic conditions: American Mineralogist, v. 98, no. 1, p. 163–180.

Snyder, R. L., and Bish, D. L., 1989, Quantitative analysis, *in* Bish, D.L., and Post, J.E., eds., Modern Powder Diffraction: Reviews in Mineralogy, v. 20, Mineralogical Society of America, p. 101–144.

Środoń, J., Drits, V. A., McCarty, D. K., Hsieh, J. C. C., and Eberl, D. D., 2001, Quantitative X-ray diffraction analysis of clay-bearing rocks from random preparations: Clays and Clay Minerals, v. 49, no. 6, p. 514–528.

Strobl, C., Malley, J., and Tutz, G., 2009, An introduction to recursive partitioning: rationale, application, and characteristics of classification and regression trees, bagging, and random forests: Psychological Methods, v. 14, no. 4, p. 323.

Taylor, K. G., 1990, Berthierine from the non-marine Wealden (Early Cretaceous) sediments of south-east England: Clay Minerals, v. 25, no. 3, p. 391–399.

Taylor, K. G., and Curtis, C. D., 1995, Stability and facies association of early diagenetic mineral assemblages: An example from a Jurassic ironstone-mudstone succession, UK: Journal of Sedimentary Research, v. 65, no. 2a, p. 358-368.
Toth, T. A., and Fritz, S. J., 1997, An Fe-berthierine from a Cretaceous laterite: Part I. Characterization: Clays and Clay Minerals, v. 45, no. 4, p. 564–579.
White, H., 1982, Maximum likelihood estimation of misspecified models: Econometrica: Journal of the Econometic Society, p. 1–25.

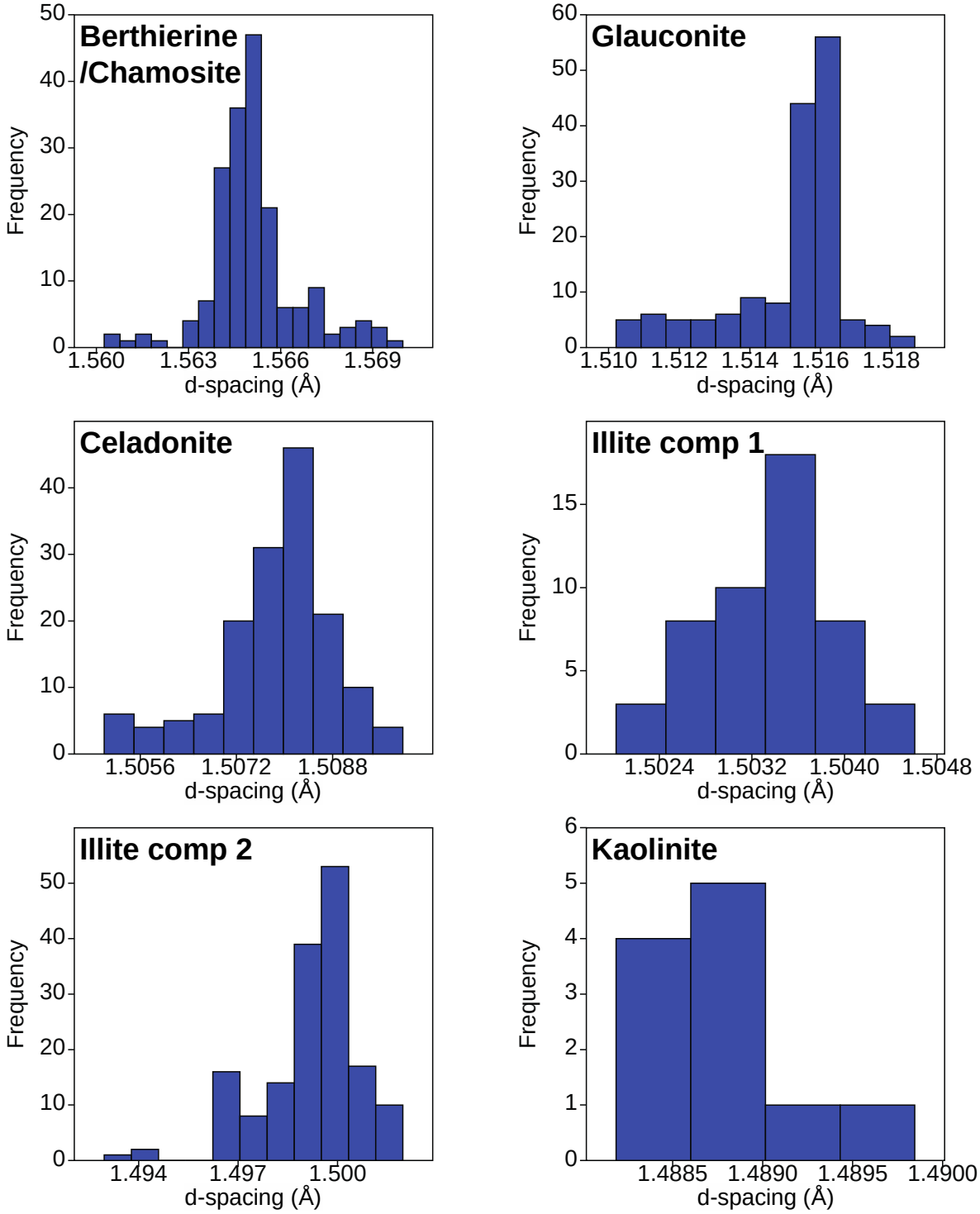

Figure DR1: Frequency distributions of d-spacing for 060 peaks of berthierine/chamosite (1.560–1570 Å), glauconite (1.510–1.519 Å), celadonite (1.505–1.510 Å), illite composition 1 (1.502–1.505 Å), illite composition 2 (1.493–1.502 Å), and kaolinite (~1.489 Å).

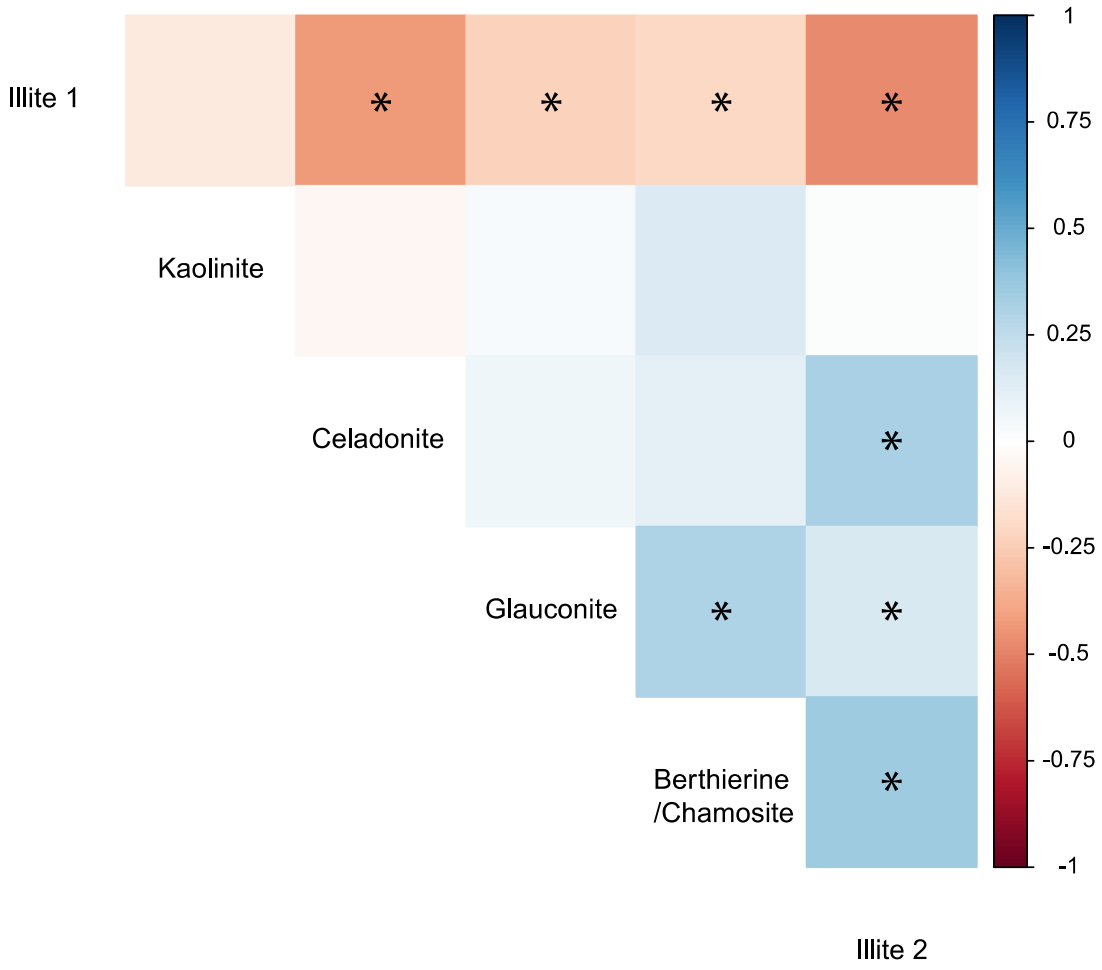

Figure DR2: Correlation matrix for the abundance of clay minerals included in the analysis. Grid colors represent Kendall's τ, and significant levels of correlation after applying Bonferroni correction are marked with an asterisk. Severe correlation between predictor variables (multicollinearity) can influence the results of a logistic regression by inflating the standard errors of the coefficients. Nonetheless, our dataset shows only moderate levels of multicollinearity which should not have a strong impact on the results (variance inflation factors for all variables ≤ 1.56).

Sample Name	Country	Stratigraphy				Contains BST fossils	Composition (% rock)								
		Formation	Member	Sequence	Height		Qtz	Calc	Dol	Bth	Gl	Cel	Il 1	Il 2	Kaol
CMj SG 0.85	USA	Marjum		Sponge Gulch	0.85	Y	34.0	22.0		9.0	5.1	11.0	0.0	7.9	0.0
CMj SG 0.93	USA	Marjum		Sponge Gulch	0.93	Y	32.0	18.0		15.6	8.9	14.1	0.0	11.4	0.0
CMj SG 0.98	USA	Marjum		Sponge Gulch	0.98	Y	36.0	25.0		9.4	5.1	13.0	0.0	10.5	0.0
CMj RW 1.26	USA	Marjum		Red Cliffs Wash	1.26	Y	31.0	19.0		7.0	7.7	18.0	0.0	15.3	0.0
CMj RW 1.28	USA	Marjum		Red Cliffs Wash	1.28	Y	32.0	17.0		8.0	5.2	16.5	0.0	18.3	0.0
CMj RW 1.38	USA	Marjum		Red Cliffs Wash	1.38	Y	30.0	14.0		7.5	7.0	15.6	0.0	16.9	0.0
CMj RW 1.44	USA	Marjum		Red Cliffs Wash	1.44	Y	28.0	12.0	4.0	8.3	4.3	17.3	0.0	19.2	0.0
CMj RW 1.82	USA	Marjum		Red Cliffs Wash	1.82	Y	25.0	16.0	5.0	6.4	8.9	15.0	0.0	19.7	0.0
CMj RW 1.92	USA	Marjum		Red Cliffs Wash	1.92	Y	41.0	8.0	8.0	10.9	2.8	7.8	0.0	14.4	0.0
CMj RW 1.96	USA	Marjum		Red Cliffs Wash	1.96	Y	34.0	9.0	8.0	7.6	3.2	8.7	0.0	21.5	0.0
CMj WHQ 1	USA	Marjum		White Hill Quarry	1.00	Y	22.0	15.0		13.3	7.3	14.2	0.0	12.2	0.0
CMj WHQ 2	USA	Marjum		White Hill Quarry	2.00	Y	37.0	21.0		6.7	7.1	11.8	0.0	9.4	0.0
CMj WHQ 3	USA	Marjum		White Hill Quarry	3.00	Y	25.0	24.0		9.4	8.5	14.0	0.0	9.1	0.0
CMj WHQ 4	USA	Marjum		White Hill Quarry	4.00	Y	23.0	25.0		10.4	9.8	12.4	0.0	9.4	0.0
CMj WHQ 5	USA	Marjum		White Hill Quarry	5.00	Y	24.0	19.0		13.0	9.6	11.8	0.0	8.5	0.0
CMj KK 7	USA	Marjum		Kell's Knolls	7.00	Y	29.0	6.0		18.2	8.8	12.2	0.0	14.8	0.0
CMj KK 9	USA	Marjum		Kell's Knolls	9.00	Y	25.0	5.0		17.5	7.1	12.0	0.0	14.5	0.0
CMj KK 11	USA	Marjum		Kell's Knolls	11.00	Y	28.0	6.0		17.5	6.1	20.4	0.0	13.0	0.0
CMj KK 13	USA	Marjum		Kell's Knolls	13.00	Y	32.0	10.0		19.2	5.7	18.3	0.0	6.8	0.0
CMj KK 16	USA	Marjum		Kell's Knolls	16.00	Y	30.0	7.0		18.5	4.9	13.5	0.0	13.1	0.0
CMj KK 18	USA	Marjum		Kell's Knolls	18.00	Y	34.0	8.0		24.8	1.0	21.6	0.0	10.7	0.0
CMj KK 20	USA	Marjum		Kell's Knolls	20.00	Y	26.0	7.0		15.0	9.5	15.3	0.0	18.1	0.0
CMj KK 24	USA	Marjum		Kell's Knolls	24.00	Y	41.0	21.0		13.2	6.1	8.2	0.0	9.6	0.0
CMj MPP 64	USA	Marjum		Marjum Pass	64.00	Y	22.0	9.0		19.3	9.1	13.9	0.0	16.7	0.0
CMj MPP 66	USA	Marjum		Marjum Pass	66.00	Y	32.0	15.0		13.7	7.5	9.2	0.0	9.5	0.0
CMj MPP 68	USA	Marjum		Marjum Pass	68.00	Y	28.0	13.0		9.7	6.0	14.4	0.0	12.9	0.0
CMj MPP 70	USA	Marjum		Marjum Pass	70.00	Y	37.0	14.0		15.2	5.1	18.2	0.0	7.5	0.0
CMj MPP 72	USA	Marjum		Marjum Pass	72.00	Y	37.0	23.0		4.9	5.5	7.4	0.0	5.3	0.0

Sample Name	Country	Stratigraphy				Contains BST fossils	Composition (% rock)								
		Formation	Member	Sequence	Height		Qtz	Calc	Dol	Bth	Gl	Cel	Il 1	Il 2	Kaol
CMj MPP 74	USA	Marjum		Marjum Pass	74.00	Y	41.0	25.0		4.3	5.1	7.5	0.0	5.1	0.0
CW 3	USA	Wheeler		Marjum Pass - Lower	3.00	Y	58.0	12.0	9.0	0.0	0.0	0.0	0.0	0.0	0.0
CW 6	USA	Wheeler		Marjum Pass - Lower	6.00	Y	75.0		14.0	1.6	0.0	0.0	0.0	9.4	0.0
CW 9	USA	Wheeler		Marjum Pass - Lower	9.00	Y	37.0			25.4	15.4	0.0	0.0	22.3	0.0
CW 12	USA	Wheeler		Marjum Pass - Lower	12.00	Y	31.0	13.0	6.0	10.6	3.6	15.3	0.0	19.4	0.0
CW 15	USA	Wheeler		Marjum Pass - Lower	15.00	Y	28.0	43.0	2.0	4.0	6.5	6.0	0.0	3.6	0.0
CW 18	USA	Wheeler		Marjum Pass - Lower	18.00	Y	44.0	15.0		12.0	6.9	10.4	0.0	11.7	0.0
CW 21	USA	Wheeler		Marjum Pass - Lower	21.00	Y	34.0	14.0	2.0	13.8	6.9	10.2	0.0	14.1	0.0
CW 24	USA	Wheeler		Marjum Pass - Lower	24.00	Y	22.0	21.0		16.7	6.0	10.2	0.0	10.2	0.0
CW 27	USA	Wheeler		Marjum Pass - Lower	27.00	Y	1.0	8.0		10.2	0.0	13.0	0.0	57.8	0.0
CW 30	USA	Wheeler		Marjum Pass - Lower	30.00	Y				12.9	0.0	10.4	0.0	49.7	0.0
CW 33	USA	Wheeler		Marjum Pass - Lower	33.00	Y		78.0	7.0	0.0	0.0	0.0	0.0	0.0	0.0
CW 36	USA	Wheeler		Marjum Pass - Lower	36.00	Y	25.0	32.0		12.1	7.4	13.4	0.0	4.2	0.0
CW SSA 5	USA	Wheeler		Swasey Spring - Upper	5.00	Y	37.0	12.0		8.4	4.5	7.7	0.0	8.4	0.0
CW SSA 20	USA	Wheeler		Swasey Spring - Upper	20.00	Y	28.0	8.0	2.0	14.0	4.3	11.2	0.0	13.6	0.0
CW SSA 22	USA	Wheeler		Swasey Spring - Upper	22.00	Y	44.0	6.0		17.9	0.0	25.3	0.0	7.8	0.0
CW SSA 27	USA	Wheeler		Swasey Spring - Upper	27.00	Y	59.0	13.0		5.2	5.7	6.7	0.0	8.4	0.0
CW SSA 30	USA	Wheeler		Swasey Spring - Upper	30.00	Y	40.0	18.0		9.1	4.4	11.1	0.0	5.4	0.0
CW SSA 32	USA	Wheeler		Swasey Spring - Upper	32.00	Y	31.0	22.0		11.3	7.4	11.6	0.0	6.7	0.0
CW SSA 34	USA	Wheeler		Swasey Spring - Upper	34.00	Y	25.0	9.0		13.9	8.8	13.1	0.0	16.2	0.0
CW SSA 107	USA	Wheeler		Swasey Spring - Upper	107.00	Y	35.0	16.0		9.9	9.2	11.3	0.0	8.6	0.0
CW SSA 109	USA	Wheeler		Swasey Spring - Upper	109.00	Y	41.0	29.0		5.0	4.1	8.6	0.0	5.4	0.0

Sample Name	Country	Stratigraphy				Contains BST fossils	Composition (% rock)								
		Formation	Member	Sequence	Height		Qtz	Calc	Dol	Bth	Gl	Cel	Il 1	Il 2	Kaol
CW DMJ 26	USA	Wheeler		Drum Mountains	26.00	Y	25.0	14.0	10.0	18.1	6.1	7.7	0.0	10.1	0.0
CW DMJ 29	USA	Wheeler		Drum Mountains	29.00	Y	14.0	29.0		8.0	7.9	14.3	0.0	5.8	0.0
CW DMJ 33	USA	Wheeler		Drum Mountains	33.00	Y	35.0	13.0		12.7	6.6	8.4	0.0	11.2	0.0
CW DMJ 35	USA	Wheeler		Drum Mountains	35.00	Y	27.0	12.0	5.0	20.1	3.1	8.1	0.0	15.7	0.0
CW DMJ 44	USA	Wheeler		Drum Mountains	44.00	Y	22.0	20.0	5.0	14.4	8.1	15.4	0.0	14.2	0.0
CW DMJ 53	USA	Wheeler		Drum Mountains	53.00	Y	26.0	20.0		14.2	7.2	9.1	0.0	9.5	0.0
CW DMJ 61	USA	Wheeler		Drum Mountains	61.00	Y	29.0	32.0		9.2	0.4	13.8	0.0	5.6	0.0
CW DMJ 73	USA	Wheeler		Drum Mountains	73.00	Y	50.0	18.0		8.2	3.2	9.8	0.0	11.9	0.0
CW DMJ 73	USA	Wheeler		Drum Mountains	73.00	Y	29.0	14.0		13.6	8.9	11.7	0.0	11.7	0.0
CW DMJ 75	USA	Wheeler		Drum Mountains	75.00	Y	27.0	7.0		17.6	5.8	13.4	0.0	17.3	0.0
CK W0	China	Kaili		Wuliu-Zengjiayan	0.00	N	4.0		88.0	0.0	0.0	0.0	0.0	0.0	0.0
CK W2	China	Kaili		Wuliu-Zengjiayan	2.00	N	3.0		97.0	0.0	0.0	0.0	0.0	0.0	0.0
CK W5	China	Kaili		Wuliu-Zengjiayan	5.00	N	13.0	52.0		0.0	13.0	18.4	0.0	1.7	0.0
CK W7	China	Kaili		Wuliu-Zengjiayan	7.00	N				7.2	4.0	17.9	40.0	0.0	0.0
CK W10	China	Kaili		Wuliu-Zengjiayan	10.00	N	14.0	72.0		0.0	0.0	0.0	0.0	0.0	0.0
CK W15	China	Kaili		Wuliu-Zengjiayan	15.00	N	38.0	15.0		9.2	3.5	0.0	32.4	0.0	0.0
CK W18	China	Kaili		Wuliu-Zengjiayan	18.00	N	40.0	29.0		3.7	5.5	8.9	0.0	12.0	0.0
CK W21	China	Kaili		Wuliu-Zengjiayan	21.00	N	19.0	40.0		0.0	6.3	18.6	0.0	16.1	0.0
CK W24	China	Kaili		Wuliu-Zengjiayan	24.00	N	51.0			6.7	0.0	0.0	42.3	0.0	0.0
CK W26	China	Kaili		Wuliu-Zengjiayan	26.00	N	30.0			20.7	4.2	0.0	45.2	0.0	0.0
CK W34	China	Kaili		Wuliu-Zengjiayan	34.00	N	35.0			5.4	0.0	0.0	60.6	0.0	0.0
CK W40	China	Kaili		Wuliu-Zengjiayan	40.00	N	41.0			12.9	4.8	0.0	40.3	0.0	0.0
CK W43	China	Kaili		Wuliu-Zengjiayan	43.00	N	35.0			9.9	0.0	0.0	55.1	0.0	0.0
CK W46	China	Kaili		Wuliu-Zengjiayan	46.00	N	30.0			18.5	6.6	0.0	45.9	0.0	0.0
CK W50	China	Kaili		Wuliu-Zengjiayan	50.00	N	41.0			11.5	5.0	0.0	41.5	0.0	0.0
CK W56	China	Kaili		Wuliu-Zengjiayan	56.00	N	24.0			19.4	3.4	0.0	53.2	0.0	0.0
CK W60	China	Kaili		Wuliu-Zengjiayan	60.00	N	32.0	25.0		0.0	19.2	0.0	23.8	0.0	0.0
CK W64	China	Kaili		Wuliu-Zengjiayan	64.00	N	12.0			8.5	0.0	0.0	65.5	0.0	0.0

Sample Name	Country	Stratigraphy				Contains BST fossils	Composition (% rock)								
		Formation	Member	Sequence	Height		Qtz	Calc	Dol	Bth	Gl	Cel	Il 1	Il 2	Kaol
CK M61	China	Kaili		Miaobanpo	61.00	N	10.0			4.6	4.1	0.0	42.3	0.0	0.0
CK M65	China	Kaili		Miaobanpo	65.00	N	6.0			13.7	9.7	0.0	68.6	0.0	0.0
CK M69	China	Kaili		Miaobanpo	69.00	N	31.0			0.0	3.4	0.0	54.6	0.0	0.0
CK M71	China	Kaili		Miaobanpo	71.00	N	34.0			5.5	6.9	0.0	54.5	0.0	0.0
CK M73	China	Kaili		Miaobanpo	73.00	N	33.0			6.4	0.0	0.0	59.6	0.0	0.0
CK M76	China	Kaili		Miaobanpo	76.00	N	38.0			5.9	2.9	0.0	31.2	0.0	0.0
CK M80	China	Kaili		Miaobanpo	80.00	N	34.0			4.1	0.0	0.0	61.9	0.0	0.0
CK M83	China	Kaili		Miaobanpo	83.00	N				18.0	0.0	0.0	82.0	0.0	0.0
CK M88	China	Kaili		Miaobanpo	88.00	N	29.0			5.7	0.0	0.0	53.3	0.0	0.0
CK M90	China	Kaili		Miaobanpo	90.00	N	39.0			2.8	0.0	0.0	43.2	0.0	0.0
CK M93	China	Kaili		Miaobanpo	93.00	N	34.0			4.2	0.0	0.0	49.8	0.0	0.0
CK M96	China	Kaili		Miaobanpo	96.00	N	46.0			4.2	0.0	0.0	48.8	0.0	0.0
CK M101	China	Kaili		Miaobanpo	101.00	Y	48.0			0.0	0.0	0.0	34.0	0.0	0.0
CK M102	China	Kaili		Miaobanpo	102.00	Y	43.0			6.6	0.0	0.0	44.4	0.0	0.0
CK M104	China	Kaili		Miaobanpo	104.00	Y	38.0			11.6	0.0	0.0	50.4	0.0	0.0
CK M116	China	Kaili		Miaobanpo	116.00	Y	51.0			0.0	0.0	0.0	32.0	0.0	0.0
CK M119	China	Kaili		Miaobanpo	119.00	Y	34.0			2.7	0.0	0.0	25.3	0.0	0.0
CK M121	China	Kaili		Miaobanpo	121.00	Y	51.0			1.6	0.0	0.0	35.4	0.0	0.0
CK M126	China	Kaili		Miaobanpo	126.00	Y	36.0			3.5	0.0	0.0	43.5	0.0	0.0
CK M129	China	Kaili		Miaobanpo	129.00	N	38.0			7.1	0.0	0.0	47.9	0.0	0.0
CK M131	China	Kaili		Miaobanpo	131.00	N	34.0			0.0	0.0	39.4	0.0	25.6	0.0
CK M134	China	Kaili		Miaobanpo	134.00	N				0.0	0.0	0.0	66.0	0.0	0.0
CK M136	China	Kaili		Miaobanpo	136.00	N	39.0			0.0	0.0	29.8	0.0	31.2	0.0
CK M138	China	Kaili		Miaobanpo	138.00	N	49.0			2.2	0.0	0.0	48.8	0.0	0.0
CK M141	China	Kaili		Miaobanpo	141.00	N	34.0			0.0	0.0	0.0	57.0	0.0	0.0
CK M144	China	Kaili		Miaobanpo	144.00	N	54.0			0.0	0.0	25.6	0.0	18.4	0.0
CK M147	China	Kaili		Miaobanpo	147.00	N	40.0			0.0	0.0	27.6	0.0	32.4	0.0
CK M149	China	Kaili		Miaobanpo	149.00	N	34.0			8.0	0.0	0.0	59.0	0.0	0.0

Sample Name	Country	Stratigraphy				Contains BST fossils	Composition (% rock)								
		Formation	Member	Sequence	Height		Qtz	Calc	Dol	Bth	Gl	Cel	Il 1	Il 2	Kaol
YPM 10470	China	Shipai				N				15.5	7.9	15.5	59.1	0.0	0.0
YPM 72897	Czechoslovakia	Etage C				N	58.0			0.1	2.0	0.0	32.0	0.0	0.0
YPM 154397	UK					N	34.0			18.0	17.5	0.0	0.0	26.5	0.0
YPM 163786	USA	Pioche	Pioche D			N				0.0	0.0	16.7	0.0	83.3	0.0
YPM 203937	USA	Campito	Montenegro			N	29.0			8.0	0.0	59.0	0.0	0.0	4.0
YPM 204003	USA	Latham				N	45.0			0.0	0.0	0.0	31.7	23.3	0.0
YPM 421785	China	Balang				N	59.0			0.0	0.0	25.5	16.5	0.0	0.0
YPM 424052	USA	Rogersville				N				11.5	0.0	0.0	88.5	0.0	0.0
YPM 424072	China	Balang				N	41.0	3.0		5.9	0.0	0.0	32.1	0.0	0.0
YPM 534372	USA					N		100.0		0.0	0.0	0.0	0.0	0.0	0.0
YPM 534374	USA	Meagher				N	18.0	56.0		0.0	12.6	11.4	0.0	0.0	0.0
OUMNH A.806	UK					N				0.0	9.5	6.2	60.3	0.0	0.0
OUMNH A.1752b-A.1753a	UK					N	30.0			17.1	8.9	1.5	0.0	19.5	0.0
OUMNH A.2325a	UK					N	55.0	14.0		1.5	4.9	1.2	0.0	2.4	0.0
OUMNH A.2346a	UK					N	37.0	4.0		17.2	13.5	0.0	1.9	13.4	0.0
OUMNH A.2361	UK					N	37.0			15.3	6.6	9.8	0.0	20.3	0.0
OUMNH A.2374	UK					N	42.0			16.1	16.7	2.7	0.0	22.5	0.0
OUMNH A.2470a	UK					N	38.0			12.8	11.1	0.0	6.3	18.8	0.0
OUMNH AT.93a	Canada	Hanford Brook				N	54.0			0.0	17.9	0.0	4.5	18.6	0.0
OUMN AT.103b	Canada	Hanford Brook				N	26.0			0.0	0.0	35.6	0.0	35.4	0.0
OUMNH AX.13	Morocco					N	16.0	23.0		0.0	12.8	23.2	0.0	0.0	0.0
OUMNH AX. 19a	Morocco					N	36.0			6.4	0.0	43.6	0.0	0.0	0.0
S7C_25	Canada	Stephen				Y	34.0	9.0		20.2	9.2	5.6	0.0	9.3	7.7
S7A_0_5	Canada	Stephen				Y	17.0	13.0		22.8	8.3	12.8	0.0	12.1	0.0
S7A_4	Canada	Stephen				Y	46.0			17.4	7.7	3.3	0.0	25.6	0.0
S7A_12	Canada	Stephen				Y	27.0	8.0		19.5	7.1	4.6	0.0	33.9	0.0
S7A_8	Canada	Stephen				Y	23.0	8.0		27.2	12.0	0.0	0.0	20.8	0.0

Sample Name	Country	Stratigraphy				Contains BST fossils	Composition (% rock)								
		Formation	Member	Sequence	Height		Qtz	Calc	Dol	Bth	Gl	Cel	Il 1	Il 2	Kaol
S7A_16	Canada	Stephen				Y	33.0	3.0		22.2	8.2	0.0	0.0	28.7	0.0
S7C_4_5	Canada	Stephen				Y	33.0	36.0	12.0	4.4	4.5	5.4	0.0	4.7	0.0
S7C_6	Canada	Stephen				Y	7.0	81.0		0.1	0.3	0.5	0.0	0.0	0.0
S7C_8	Canada	Stephen				Y			54.0	0.0	0.0	0.0	0.0	0.0	0.0
S7C_10_5	Canada	Stephen				Y			36.0	2.5	15.8	15.8	0.0	0.9	0.0
S7C_12	Canada	Stephen				Y		79.0	3.0	0.0	0.0	0.0	0.0	0.0	0.0
S7C_14	Canada	Stephen				Y	30.0	24.0		18.3	5.7	6.7	0.0	11.5	1.7
S7C_14_5	Canada	Stephen				Y	31.0	24.0		16.0	4.3	7.1	0.0	8.9	1.6
S7_15	Canada	Stephen				Y	24.0	20.0		18.5	5.1	6.1	0.0	11.3	0.0
S7_17	Canada	Stephen				Y	32.0	21.0		19.0	6.8	4.0	0.0	15.4	1.8
S7_19	Canada	Stephen				Y	34.0	5.0		19.5	5.3	0.0	0.0	13.0	5.3
S7_20	Canada	Stephen				Y	56.0			16.2	4.9	0.0	0.0	19.6	2.3
S7_22	Canada	Stephen				Y	18.0	2.0	7.0	19.6	6.8	0.0	0.0	35.7	4.8
S7_27_5	Canada	Stephen				Y	41.0	12.0		19.6	8.0	0.0	0.0	11.8	5.6
CL_1	USA	Latham Shale				N	27.0			16.2	0.0	0.0	0.0	47.8	0.0
CL_2	USA	Latham Shale				N	50.0			0.0	0.0	9.3	0.0	31.7	0.0
CL_3	USA	Latham Shale				N	40.0			0.0	0.0	7.1	0.0	43.9	0.0
CL_4	USA	Latham Shale				N	34.0			0.0	0.0	10.5	0.0	38.5	0.0
CL_5	USA	Latham Shale				N	33.0			0.0	0.0	6.4	0.0	60.6	0.0
CL_6	USA	Latham Shale				N	21.0			0.0	0.0	11.8	0.0	57.2	0.0
CPH_1	USA	Carrara				N				20.9	0.0	32.5	0.0	46.6	0.0
CPH_2	USA	Carrara				N	36.0	7.0		12.8	3.7	16.4	0.0	25.0	0.0
CPH_3	USA	Carrara				N	18.0			21.7	0.0	19.5	0.0	37.8	0.0
CPH_4	USA	Carrara				N				28.8	0.0	29.5	0.0	41.7	0.0
CPH_5	USA	Carrara				N	27.0			15.7	3.4	18.2	0.0	30.7	0.0
FP_1	Canada	Stephen	Burgess			Y		7.0	6.0	26.0	1.6	18.5	0.0	30.9	0.0

Sample Name	Country	Stratigraphy				Contains BST fossils	Composition (% rock)								
		Formation	Member	Sequence	Height		Qtz	Calc	Dol	Bth	Gl	Cel	Il 1	Il 2	Kaol
FP_2	Canada	Stephen	Burgess			Y	16.0	10.0		21.0	3.2	20.3	0.0	20.5	0.0
FP_3_7	Canada	Stephen	Burgess			Y	30.0	12.0		28.0	3.0	10.7	0.0	16.3	0.0
FP_4_9	Canada	Stephen	Burgess			Y	27.0	15.0	2.0	17.4	3.6	10.0	0.0	14.0	0.0
FP_6	Canada	Stephen	Burgess			Y	20.0	16.0		13.8	4.8	11.1	0.0	13.3	0.0
FP_7	Canada	Stephen	Burgess			Y	18.0	15.0		23.4	8.0	11.4	0.0	16.1	0.0
FP 8_9	Canada	Stephen	Burgess			Y		4.0	25.0	1.4	0.7	9.3	0.0	31.6	0.0
FP_9	Canada	Stephen	Burgess			Y	26.0	24.0		8.5	4.7	8.8	0.0	8.0	0.0
FP_10	Canada	Stephen	Burgess			Y	12.0	69.0	6.0	0.2	0.9	2.0	0.0	0.0	0.0
FP_11	Canada	Stephen	Burgess			Y	15.0	63.0	2.0	0.0	0.0	0.0	0.0	0.0	0.0
FP_12	Canada	Stephen	Burgess			Y	19.0	21.0	5.0	15.4	7.8	11.4	0.0	11.4	0.0
FP_20	Canada	Stephen	Burgess			Y	17.0	8.0	15.0	17.5	5.3	6.7	0.0	24.5	0.0
FP_20_5	Canada	Stephen	Burgess			Y	27.0	3.0		25.7	0.0	5.5	0.0	26.8	0.0
FP_21_8	Canada	Stephen	Burgess			Y	36.0			19.4	9.3	11.7	0.0	12.6	0.0
FP_22	Canada	Stephen	Burgess			Y	15.0	25.0		15.4	14.6	14.3	0.0	9.7	0.0
FP_23	Canada	Stephen	Burgess			Y	17.0	11.0	14.0	11.0	5.6	12.0	0.0	22.4	0.0
FP_24	Canada	Stephen	Burgess			Y	27.0	31.0		7.8	7.3	7.6	0.0	3.3	0.0
FP_25	Canada	Stephen	Burgess			Y	21.0	28.0		11.1	8.0	9.0	0.0	6.9	0.0
FP_26	Canada	Stephen	Burgess			Y	30.0	6.0		23.3	4.2	5.4	0.0	13.1	0.0
FP_27	Canada	Stephen	Burgess			Y	28.0	16.0		12.6	4.5	11.6	0.0	7.2	0.0
FP_28	Canada	Stephen	Burgess			Y	39.0	6.0		17.0	3.3	4.8	0.0	19.0	0.0
FP_30	Canada	Stephen	Burgess			Y		9.0	1.0	26.2	12.2	9.5	0.0	29.0	0.0
FP_31	Canada	Stephen	Burgess			Y	22.0	26.0		11.3	6.5	7.6	0.0	9.7	0.0
FP_32	Canada	Stephen	Burgess			Y		9.0	2.0	16.8	21.7	2.5	0.0	32.0	0.0
FP_33	Canada	Stephen	Burgess			Y	4.0	2.0		14.0	0.0	24.7	0.0	47.3	0.0
FP_35	Canada	Stephen	Burgess			Y	18.0	5.0		20.9	11.6	4.0	0.0	27.5	0.0
FP_36	Canada	Stephen	Burgess			Y	28.0	2.0		21.3	10.5	0.0	0.0	31.1	0.0
FP_37	Canada	Stephen	Burgess			Y	37.0	3.0		11.2	9.8	0.0	0.0	24.0	0.0
FP_38	Canada	Stephen	Burgess			Y	19.0	8.0		21.9	7.3	3.9	0.0	27.9	0.0

Sample Name	Country	Stratigraphy				Contains BST fossils	Composition (% rock)								
		Formation	Member	Sequence	Height		Qtz	Calc	Dol	Bth	Gl	Cel	Il 1	Il 2	Kaol
FP_39	Canada	Stephen	Burgess			Y	27.0	14.0		16.0	8.8	9.9	0.0	24.4	0.0
OWC_0_12	USA	Pioche				N	37.0			15.6	9.0	0.0	0.0	30.4	0.0
OWC_0_28	USA	Pioche				N	26.0			16.5	7.5	12.5	0.0	28.5	0.0
OWC_0_32	USA	Pioche				N	24.0			17.6	9.8	12.9	0.0	28.7	0.0
OWC_0_38	USA	Pioche				N	22.0			20.9	11.1	5.8	0.0	40.2	0.0
OWC_1	USA	Pioche				Y	24.0			0.0	0.0	15.7	0.0	59.3	0.0
RW_1	USA	Pioche				N	30.0			17.2	0.0	28.0	0.0	24.9	0.0
RW_2	USA	Pioche				N	24.0			20.6	0.0	14.7	0.0	34.7	0.0
RW_3	USA	Pioche				N	44.0			9.9	0.0	18.8	0.0	21.3	0.0
RW_4	USA	Pioche				N	40.0	3.0		13.0	1.6	16.5	0.0	26.0	0.0
RW_5	USA	Pioche				N	27.0			15.3	0.0	16.9	0.0	40.8	0.0
RW_6	USA	Pioche				N				23.4	3.1	24.9	0.0	48.5	0.0
WHY_S_41	Canada	Stephen	Burgess			Y	68.0		6.0	0.0	0.0	0.0	0.0	0.0	0.0
WHY_S_43	Canada	Stephen	Burgess			Y		42.0	31.0	0.0	0.0	0.0	0.0	0.0	0.0
WHY_S_47	Canada	Stephen	Burgess			Y	18.0	4.0		32.9	5.5	9.2	0.0	20.4	0.0
WHY_S_51	Canada	Stephen	Burgess			Y	24.0	7.0		27.5	3.2	8.5	0.0	20.8	0.0
WHY_S_53	Canada	Stephen	Burgess			Y	34.0	36.0		7.0	7.4	7.1	0.0	4.4	0.0
WHY_S_55	Canada	Stephen	Burgess			Y	17.0	19.0	3.0	19.2	8.4	10.8	0.0	11.6	0.0
WHY_S_45_(5)	Canada	Stephen	Burgess			Y		53.0	12.0	0.0	0.0	0.0	0.0	0.0	0.0
YPM 200359	USA	Wheeler				Y	28.0	40.0		8.4	6.7	7.6	7.3	0.0	0.0
YPM 219298	Canada	Stephen				Y	33.0	5.0	2.0	13.0	16.3	0.0	0.0	19.7	0.0
YPM 424000	China	Kaili				Y	47.0			9.2	3.4	0.0	40.3	0.0	0.0
YPM 529546	USA	Langston	Spence			Y		6.0		26.6	10.9	2.9	0.0	47.7	0.0
YPM 533117	USA	Wheeler				Y	25.0	20.0		13.1	5.9	15.4	0.0	10.6	0.0
YPM 534367	Canada	Stephen	Burgess			Y	33.0	9.0		12.1	17.0	0.0	0.0	26.9	0.0
YPM 14392	USA	Kinzers				Y	18.0			11.7	0.0	62.8	0.0	2.7	4.8

Table DR1: Sample identifications and mineralogical composition. Abbreviations: Qtz = quartz, Calc = calcite, Dol = dolomite, Bth = berthierine/chamosite, Gl = glauconite, Cel = celadonite, Il 1 = illite composition 1, Il 2 = illite composition 2, Kaol = kaolinite.